Vol 15 No 6, June 2006
1009-1963/2006/15(06)/1391-07

Chinese Physics

© 2006 Chin. Phys. Soc.
and IOP Publishing Ltd

Systematical study of the trapping forces of optical tweezers formed by different types of optical ring beams*

Xu Sheng-Hua(徐升华)[a)b)], Li Yin-Mei(李银妹)[a)b)†], and Lou Li-Ren(楼立人)[b)‡]

[a)] *National Laboratory for Physical Sciences at Microscale, University of Science and Technology of China, Hefei* 230026, *China*

[b)] *Department of Physics, University of Science and Technology of China, Hefei* 230026 *China*

(Received 6 July 2005; revised manuscript received 24 February 2006)

The technique of optical tweezers has been improved a lot since its invention, which extends the application fields of optical tweezers. Besides the conventionally used Gaussian beams, different types of ring beams have also been used to form optical tweezers for different purposes. The two typical kinds of ring beams used in optical tweezers are the hollow Gaussian beam and Laguerre–Gaussian (LG) beam. Both theoretical computation and experiments have shown that the axial trapping force is improved for the ring beams compared with the Gaussian beam, and hence the trapping stability is improved, although the transverse trapping forces of ring beams are smaller than that of Gaussian beam. However, no systematic study on the trapping forces of ring beam has ever been discussed. In this article, we will investigate the axial and transverse trapping forces of different types of ring beams with different parameters systematically, by numerical computation in which the ray optics model is adopted. The spherical aberration caused by the refractive index mismatch between oil and water is also considered in the article. The trapping forces for different objectives that obey the sine condition and tangent condition are also compared with each other. The result of systematical calculation will be useful for the applications of optical tweezers formed by different types of ring beams.

Keywords: optical tweezers, trapping force, spherical aberration
PACC: 9430H, 4215, 3280P

1. Introduction

Optical tweezers[1,2] have found practical applications in various fields of science, such as biology[3−5] and colloid chemistry,[6−9] etc, since their invention. Different techniques of optical tweezers have been developed, such as scanning optical tweezers[10] and dual optical tweezers,[11] for applications in different cases. To find a better beam intensity distribution for improving the trapping efficiency of optical tweezers, ring beams have been used to form optical tweezers, based on the understanding that the central part of a beam contributes more scattering force than gradient force. Until now, the two typical ring beams used are the hollow Gaussian beam formed by blocking the centre of the Gaussian mode beam,[12] and the Laguerre–Gaussian (LG) mode optical beam. The axial trapping forces of the hollow Gaussian beam have already been calculated.[13] O'Neil and Padgett[14] compared the axial and transverse trapping forces of LG mode with those of the Gaussian mode experimentally. They also carried out some numerical calculations to support the experiment result.

As discussed before,[12−14] both types of ring beams an increase the axial trapping force, as compared with Gaussian beam. However, some researchers showed that the hollow Gaussian beam may reduce the transverse trapping efficiency.[15,16] For LG mode beams, the trapping forces of individual rays in an optical tweezers were calculated for interpreting the experimental result in Ref.[14]. Since the above calculation only considered some individual rays, it cannot give a full image of the transverse force of the

*Project supported by the National Natural Science Foundation of China (Grant Nos 20273065 and 10474094) and 'the Knowledge Innovation Program' of Chinese Academy of Sciences.

†E-mail: liyinmei@ustc.edu.cn
‡E-mail: loulr@ustc.edu.cn

LG mode.

The effect of spherical aberration is known qualitatively within the community of users of optical tweezers.[17,18] To understand the effect quantitatively, some researchers[18−21] studied the influence of spherical aberration on the trapping of spherical particles both theoretically and experimentally. However, the spherical aberration has not been introduced in the study of the optical tweezers formed by ring beams.

In the calculation of the trapping forces using ray optics(RO) model, different considerations of the microscope objective will give different calculated result. Some studies considered that the microscope objective adheres to the tangent condition (with a flat exit pupil),[20] while others considered that the objective adheres to the sine condition (with a curved exit pupil),[21] which is believed suitable for most objectives. The different considerations of objectives will also cause the difference of the trapping force calculated.

In this paper, we will calculate the axial and transverse trapping forces systematically for the hollow Gaussian beam and LG beam to show that how the intensity distribution of the beam influences the trapping forces. The RO model[2] is used in the calculation. The influence of the spherical aberration resulting from the refractive index mismatch between the oil and the suspending medium of particles on the trapping force[19−21] has also been included in the calculation. And the trapping forces for the objectives under the sine condition and tangent condition are compared in this paper.

2. Calculation of the trapping force

Using the RO model, the total force exerted on a particle can be obtained by calculating the forces of single rays that strike the particle and then integrating them. According to Fresnel laws, an incident ray on a particle will be partly transmitted through and partly reflected form the particle surface. Each refraction and reflection will transfer momentum and exert force to the particle. The principal relationship between the trapping force and power is $F = QnP/c$, where n is the refractive index of the surrounding medium, P is the laser power, and c is the speed of light in free space. Q is a normalized trapping force, which is generally named as trapping efficiency.

It was shown by Ashkin[2] that the force produced by a single ray that impinges upon a bead can be divided into two parts, ray-scattering force parallel to the incident ray, and ray-gradient force perpendicular to the incident ray. The trapping efficiency of the two parts can be written as

$$Q_{\rm s} = 1 + R\cos(2\theta) - \frac{T^2[\cos(2\theta - 2r) + R\cos(2\theta)]}{1 + R^2 + 2R\cos(2r)}, \quad (1)$$

$$Q_{\rm g} = R\sin(2\theta) - \frac{T^2[\cos(2\theta - 2r) + R\sin(2\theta)]}{1 + R^2 + 2R\cos(2r)}, \quad (2)$$

where θ is the angle of incidence, r is the angle of refraction, R and T are the Fresnel reflection and transmission coefficients, respectively. Figure 1 shows the geometry of the light propagation in a system with a bead in a uniform medium.

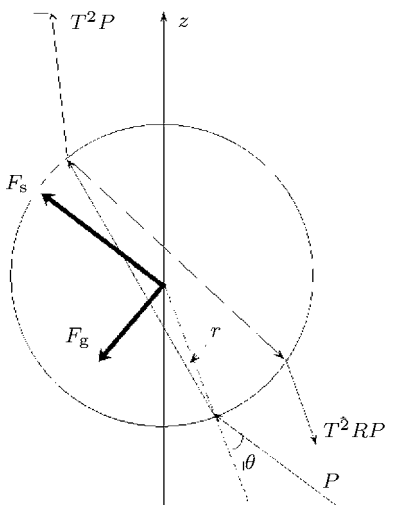


Fig.1. RO model for optical trapping (after Ashkin[2]). The ray-scattering force $F_{\rm s}$ points to the direction of the incident ray, while the gradient force $F_{\rm g}$ is perpendicular to the direction of the incident ray. θ is the angle of incidence, r is the angle of refraction. The intensities of the reflected and refracted rays are determined by the Fresnel reflection coefficient R and transmission T coefficient, and by the power P of the incident ray.

For axial trapping the bead is thought to be on the axis and the summation of the forces of all the rays is not too difficult. In Ref.[21], the axial trapping force for Gaussian beam was calculated using RO model by taking the spherical aberration into consideration. In this paper, calculation of the axial trapping forces is similar. The difference is that the intensity distributions of the hollow Gaussian beam and the LG beam are different from the Gaussian beam. In Ref.[21], the objectives obey the sine condition. For the objectives obeying the tangent condition, some geometric parameters need to be changed accordingly. The same

consideration is taken for the calculation of the transverse trapping force for beams of different intensity distributions and for objectives obeying sine and tangent conditions. However, since the bead is off axis in this case, the geometrical analysis of the ray trace is much more complicated than that in the case of axial trapping, which will be discussed in the following paragraphs.

Suppose that an ideal oil immersion objective is used, a light beam coming out from the objective forms a light cone in index matching medium of oil–glass. The apex of the cone is point O in Fig.2, which would be the focus point of the laser beam if the medium after the objective had a uniform refractive index of oil. The point O is taken as the origin of the coordinate system. The z axis in the figure is along

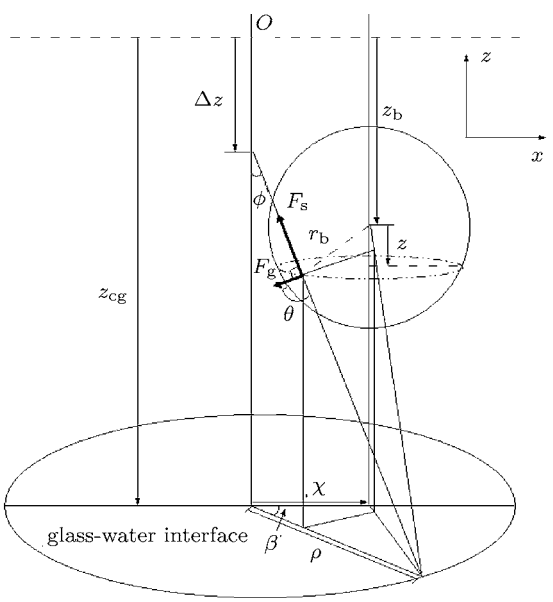


Fig.2. Schematic illustration of light impinging on an off-axis particle in an optical tweezers system including a glass-water interface. O is the origin, which is the ideal focus point of the beam in the oil-glass media. In the figure, F_s and F_g indicate only the directions of the scattering force and the gradient force on the particle. The parameters in the figure are used in the calculation and are discussed in the text.

the direction of propagation of the beam, which is upward and perpendicular to the glass-water interface. The direction of x axis is taken to be along the transverse displacement of the particle for simplicity. The position of the glass-water interface is denoted as z_{cg} which lies between O and the interface. In a typical experiment with optical tweezers, the light passes through immersion oil and glass before it enters water. The oil and glass are supposed to have identical refraction indices n_g, while the index of refraction of water is n_w, which is lower than n_g. This index mismatch causes the spherical aberration, which can be considered automatically through ray tracing. When the beam passes the interface between oil-glass and water, all the rays of the beam are refracted. Each ray propagates along its own refracted direction at an angle ϕ with respect to the axis and intersects the axis at a point Δz apart from the point O, as shown in Fig.2. For a typical ray in the figure, β is the angle of the projection of the incident beam on the glass-water interface with respect to the x direction. Now considering a bead of radius r_b in the light field, its axial position relative to the point O is z_b and the transverse position away from the axis is x. The incident beam and the normal on the particle form a main plane. The directions of scattering and gradient forces F_s and F_g are both in the main plane, which is also shown in Fig.2.

For a single ray, which comes out of the exit pupil of the objective at a radial coordinate ρ, η is defined as the relative pupil coordinate in terms of the radius of the exit pupil, ρ_p, as

$$\eta = \frac{\rho}{\rho_p}. \tag{3}$$

By geometrical reasoning, Δz can be written as

$$\Delta z = z_{cg}\left\{1 - \frac{n_w}{n_g}\left[\frac{1-\eta^2\left(\frac{NA}{n_w}\right)^2}{1-\eta^2\left(\frac{NA}{n_g}\right)^2}\right]^{1/2}\right\}, \tag{4}$$

where NA is the numerical aperture of the objective.

The relationship between ϕ and η under sine condition can be different from that under tangent condition. It can be written as

$$\sin(\phi) = \frac{NA}{n_w}\eta, \tag{5}$$

for the sine condition, and

$$\sin(\phi) = \left(\frac{n_g}{n_w}\right)\sin\left(\tan^{-1}\left\{\eta\tan\left[\sin^{-1}\left(\frac{NA}{n_g}\right)\right]\right\}\right), \tag{6}$$

for the tangent condition. These two equations will also be used in the calculation of axial trapping force.

For the ray shown in Fig.2, the vertical distance z between the bead centre and the incident point on the bead surface can be deduced from the above mentioned parameters as

$$z = \frac{-\sqrt{(2(z_b-\Delta z)\tan^2\phi + 2x\tan\phi\cos\beta)^2 - 4(\tan^2\phi+1)((z_b-\Delta z)^2\tan^2\phi + x^2 + 2x(z_b-\Delta z)\tan\phi\cos\beta - r_b^2)}}{2(\tan^2\phi+1)} - \frac{(2(z_b-\Delta z)\tan^2\phi + 2x\tan\phi\cos\beta)}{2(\tan^2\phi+1)}. \quad (7)$$

The intersection point of the beam on the particle surface, the centre of the particle and the intersection point of the incident beam with the glass–water interface, form a triangle. From the parameters mentioned above, the lengths of the three sides of the triangle can be deduced by geometrical reasoning. Then the incident angle θ at the bead surface can be calculated. Using Eqs.(1) and (2), the scattering force and gradient force can be calculated.

To calculate the transverse force, it is also needed to calculate the projection of the forces in the x direction. The directions of the scattering and gradient forces are shown in Fig.2. Using the above-mentioned parameters, the projection angles of F_s and F_g made with x axis can also be deduced by geometrical analysis.

Then the transverse force due to the single ray can be calculated using the above equations and analysis with the given system parameters $n_g, n_w, NA, z_b, z_{cg}, r_b, x, \beta$, and η. The total transverse force can be calculated by integrating the forces of the single rays.

In this paper, two different types of ring beams are concerned. The first type is the hollow Gaussian beam formed by blocking the centre of the Gaussian beam. The beam is assumed to have a truncated and hollow Gaussian intensity distribution at the position of the exit pupil, $I(\rho)$, given by

$$I(\rho) = \begin{cases} I_0\exp(-2\rho^2/\omega_0^2) & \rho_h \le \rho \le \rho_p; \\ 0 & \rho > \rho_p \quad \text{or} \quad \rho < \rho_h, \end{cases} \quad (8)$$

where I_0 is the intensity at the centre of the Gaussian beam, ω_0 is the width of the beam at the exit pupil of the objective, ρ_p is the radius of the exit pupil, ρ_h is the radius of the hollow. In the calculation followed, we take ω_0 equal to ρ_p.

For LG beam, the field amplitude can be described in cylindrical coordinates as[22]

$$u_{pl}(\rho,\varphi,z) = \frac{C}{(1+z^2/z_R^2)^{1/2}}\left(\frac{\rho\sqrt{2}}{\omega(z)}\right)^l L_p^l\left(\frac{2\rho^2}{\omega^2(z)}\right)\exp\left(\frac{-\rho^2}{\omega^2(z)}\right) \times \exp\frac{-ik\rho^2 z}{2(z^2+z_R^2)}\exp(-il\varphi)\exp\left(i(2p+l+1)\tan^{-1}\frac{z}{z_R}\right), \quad (9)$$

where z_R is the Rayleigh range, $\omega(z)$ is the radius of the beam, L_p^l is the associated Laguerre polynomial, C is a constant, and the beam waist is at $z = 0$.

Then the intensity distribution at the exit pupil can be written as

$$I(\rho) = \begin{cases} C_0\left(\frac{\rho\sqrt{2}}{\omega_0}\right)^{2l}\left(L_p^l\left(\frac{2\rho^2}{\omega_0^2}\right)\right)^2\exp\left(\frac{-2\rho^2}{\omega_0^2}\right) & \rho \le \rho_p; \\ 0 & \rho > \rho_p, \end{cases} \quad (10)$$

where $\omega_0 = \omega(z_{ep})$ is the radius of the beam at the exit pupil of the objective, ρ_p is the radius of the exit pupil. C_0 is another constant related to C. In the following calculation, we take ω_0 equal to ρ_p, which is the same as the calculation in the case of the hollow Gaussian beam.

For different types of the light beam, the trapping points may be different. To make the results comparable, the trapping points of the particle for different types of beams are first calculated. Then the transverse trapping force is calculated for the particle departed from the trapping point transversely.

3. Results

In the calculation, the spherical particles have a refractive index of 1.55. The refractive index of water is 1.33. The indices of refraction of glass and immersion oil are taken to be 1.516. NA is a constant taken to be 1.25. As a typical case, z_{cg} is taken to be $-6r_b$ in the calculation, where r_b is the radius of the particle. The axial and transverse trapping forces depend on the relative sizes of the particle, the beam and its central shadow (or the order for LG mode) are calculated for the different intensity distributions of the hollow Gaussian beam and the LG beam. The objectives obeying sine condition and tangent condition are also compared with each other.

Figures 3 and 4 show the transverse trapping efficiencies for ring beams of the hollow Gaussian mode beam and the LG beam, respectively, as compared with that of Gaussian beam, for the objectives obeying the sine condition. Figures 5 and 6 are the transverse trapping efficiencies for the objectives obeying the tangent condition. Figures 7 and 8 are the axial trapping efficiencies for the objectives obeying the sine condition, while Figs.9 and 10 are for the objectives obeying the tangent condition. For Figs.3–6, the reference points for the transverse displacements are the trapping positions. For Figs.7–10, the axial position is relative to the point O. In the figures, the radius of the hollow of the hollow Gaussian beam takes values 0.2, 0.4, 0.6 and $0.8\omega_0$, and the order l of the LG beam, as shown in Eg.(10), takes values 1, 2, 3, and 4.

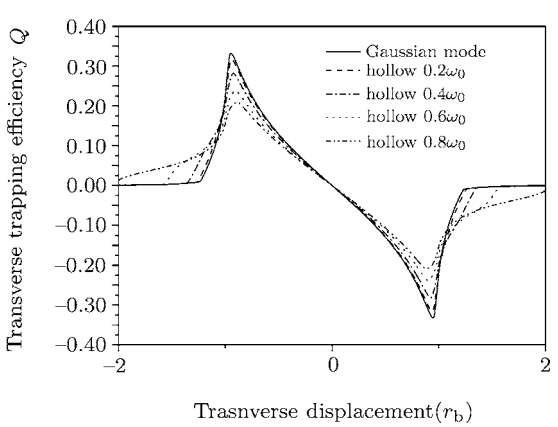


Fig.3. The transverse trapping force vs. the transverse displacement from the trapping positions, for hollow Gaussian beams with different radius of the hollow, compared with the transverse force for the Gaussian beam. The objectives obey the sine condition.

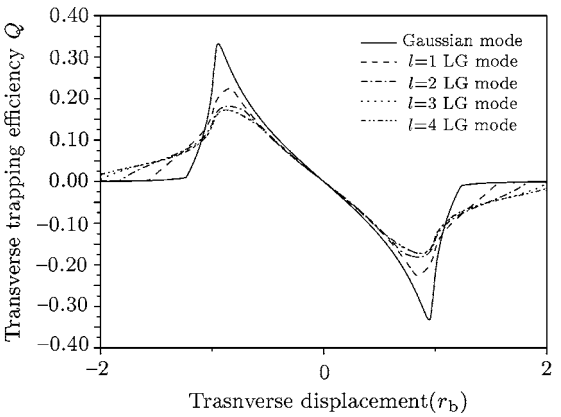


Fig.4. The transverse trapping force vs. the transverse displacement from the trapping positions, for Laguerre–Gaussian beams with different orders l, compared with the transverse force for the Gaussian beam. p is taken to be 0. The objectives obey the sine condition.

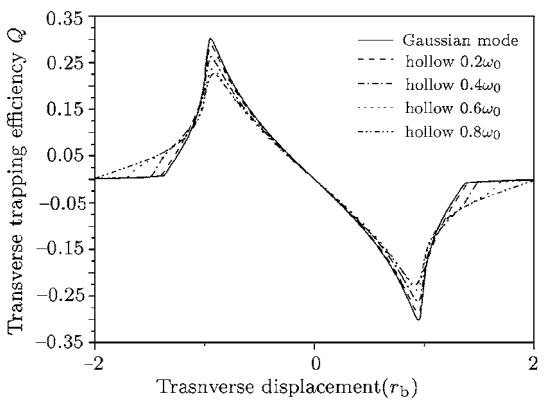


Fig.5. The transverse trapping force vs. the transverse displacement from the trapping positions, for hollow Gaussian beams with different radius of the hollow, compared with the transverse force for the Gaussian beam. The objectives obey the tangent condition.

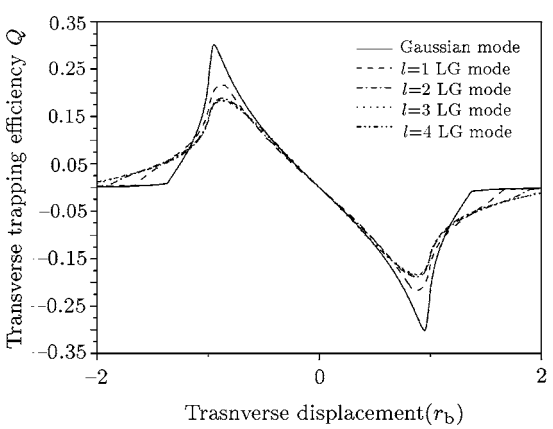


Fig.6. The transverse trapping force vs. the transverse displacement from the trapping positions, for Laguerre–Gaussian beams with different orders l, compared with the transverse force for the Gaussian beam. p is taken to be 0. The objectives obey the tangent condition.

Since the spherical aberration is taken into consideration in this paper, the laser beam cannot converge into an ideal focus in the medium, so the axial trapping forces are not symmetrical, and the equilibrium points for different kind of beams are different. From Figs.7–10 we can see that as the hollow radius of the hollow Gaussian beam and/or the order of the LG beam increases, the numerical value of the axial positions of the equilibrium points becomes smaller, indicating that the axial trapping positions move along the negative z direction. The difference of the trapping positions for Gaussian beam compared with the 0.8 hollow beam and the fourth order LG beam can be nearly $1r_b$. The figures also show that the maximum trapping force in the negative z direction is larger than that in the positive z direction. Therefore, it will be easier for particles to escape from the optical trap along the positive z direction than along the negative z direction, which is consistent with the experimental results. To increase the trapping stability, it is more important to increase the maximum trapping forces in the positive z direction. The results of Figs.7–10 show that when the hollow radius of the hollow Gaussian beam and(or) the order of the LG beam increases, the axial trapping forces in the positive z direction increase. The increase of the axial trapping force can be up to 2–3 times for the high-order ring beams compared with the Gaussian beam, indicating that the ring beams greatly improve the stability of the optical trapping. The results also indicate that for the objective obeying sine condition, compared with the tangent objective, the maximum trapping force on positive z side increases more rapidly with the hollow size of the ring beam. However, Figs.3–6 show that the ring beams decrease the transverse trapping forces,

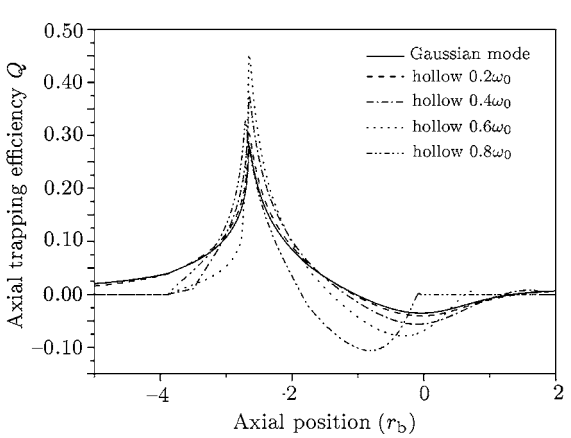


Fig.7. The axial trapping force vs. the axial positions, for hollow Gaussian beams with different radius of the hollow, compared with the axial force for Gaussian beam. The objectives obey sine condition.

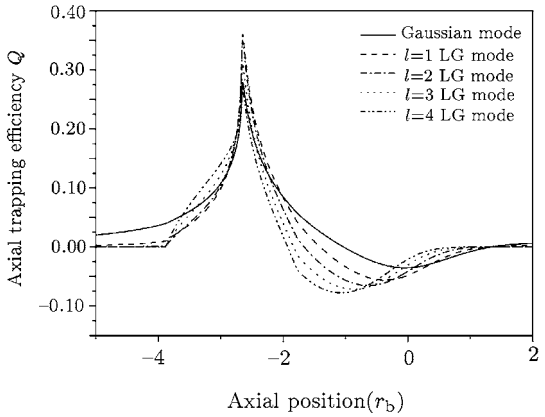


Fig.8. The axial trapping force vs. the axial positions, for Laguerre–Gaussian beams with different orders l, compared with the axial force for Gaussian beam. p is taken to be 0. The objectives obey the sine condition.

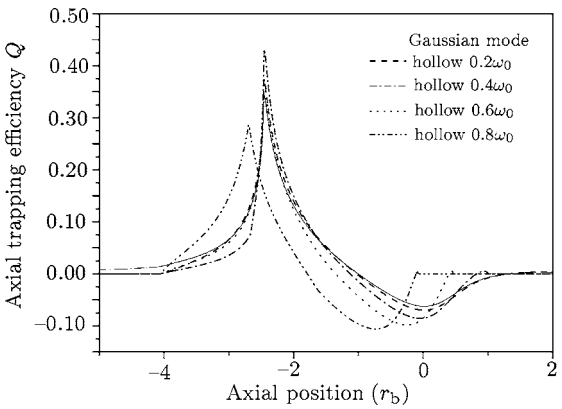


Fig.9. The axial trapping force vs. the axial positions, for hollow Gaussian beams with different radius of the hollow, compared with the axial force for Gaussian beam. The objectives obey the tangent condition.

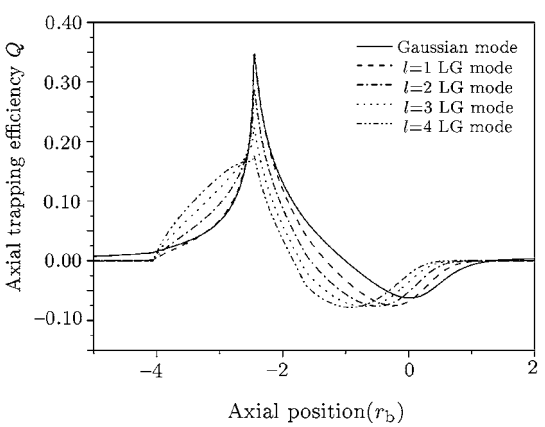


Fig.10. The axial trapping force vs. the axial positions, for Laguerre-Gaussian beams with different orders l, compared with the axial force for Gaussian beam. p is taken to be 0. The objectives obey the tangent condition.

which means that the ring beams sacrifice the transverse trapping force for improving the axial trapping stability.

4. Discussion and conclusion

For different types of ring beams, the axial and transverse trapping forces have been calculated and compared with each other in this paper. The spherical aberration resulting from the refractive index mismatch between the oil and the suspending medium for particles are taken into consideration in the calculation, and the trapping forces for the objectives obeying the sine condition and tangent condition are also compared in this paper. The calculated results show that the two commonly used ring beams, hollow Gaussian beam and LG beam, both increase the axial trapping efficiency but decrease the transverse trapping efficiency with the increase of hollow size or LG beam order.

The result can be qualitatively explained by the different intensity distributions of the Gaussian mode, LG mode, and hollow Gaussian beams. For axial trapping, the gradient force of the rays near the beam axis is smaller, while the scattering force is larger as compared with the rays far from the beam axis. So the ring beams can increase the axial trapping force, which is the most important for trapping stability because the axial trapping force is usually an order of magnitude weaker than the transverse one.

However, for the transverse trapping, the particle is far from the trapping position transversely, so that the rays near the beam axis will exert forces pointing to the trapping position. If the intensity is small in the centre, as the ring beams are, the restoring force pointing to the trapping position will be small, which causes the Gaussian beam to have larger transverse trapping force than the ring beams.

For the objectives obeying the sine condition and the tangent condition, the geometrical parameters of the rays incident on the particle are different, which causes the results to be different quantitatively. In theoretical calculation of the trapping of optical tweezers, the parameters of the objectives should be chosen appropriately to obtain more precise result.

From the calculated result, we see that it would be better to use the ring beams for the application when the transverse trapping force is of minor importance. Since LG mode beam has orbital angular momentum, which can make some absorptive particles rotate, the angular momentum will increase with the beam order. It can be concluded that in the applications where the high angular momentum is needed, the mode order of the LG beam has to be chosen properly to gain adequate angular momentum and transverse trapping force. We think the results obtained in this paper will be helpful for different kinds of experiments and applications of optical tweezers, where different trapping characters may be needed.

References

[1] Ashkin A, Dziedzic J M, Bjorkholm J E and Chu S 1986 *Opt. Lett.* **11** 288

[2] Ashkin A 1992 *Biophys. J.* **61** 569

[3] Ashkin A and Dziedzic J M 1987 *Science* **235** 1517

[4] Ishijima A, Kojima H, Funatsu T, Tokunaga M, Higuchi H, Tanaka H and Yanagida T 1998 *Cell* **92** 161

[5] Wang M D 1999 *Curr. Opin. Biotechno.* **10** 81

[6] Crocker J C 1997 *J. Chem. Phys.* **106** 2837

[7] Crocker J C and Grier D G 1994 *Phys. Rev. Lett.* **73** 352

[8] Grier D G 1997 *Curr. Opin. Colloid Interface Sci.* **2** 264

[9] Owen R J, Crocker J C, Verma R and Yodh A G 2001 *Phys. Rev.* E **64** art. No.11401

[10] Sasaki K, Koshio M, Misawa H, Kitamura N and Masuhara H 1991 *Opt. Lett.* **16** 1463

[11] Fallman E and Axner O 1997 *Appl. Opt.* **36** 2107

[12] Yin L H, Li Y M, Lou L R, Zhang D and Chen H T 2003 *Chin. J. Lasers.* **30** 211 (in Chinese)

[13] Cui G Q, Li Y M, Weng M Q and Lou L R 2001 *Chin. J. Lasers* **28** 89 (in Chinese)

[14] O'Neil A T and Padgett M J 2001 *Opt. Commun.* **193** 45

[15] Gu M, Morrish D and Ke P C 2000 *Appl. Phys. Lett.* **77** 34

[16] Ganic D, Gan X and Gu M 2005 *Opt. Express* **13** 1260

[17] Wright W H, Sonek G J and Berns M W 1994 *Appl. Opt.* **33** 1735

[18] Ke P C and Gu M 1998 *J. Mod. Opt.* **45** 2159

[19] Rohrbach A and Stelzer E H K 2002 *Appl. Opt.* **41** 2494

[20] Yao X C, Li Z L, Guo H L, Cheng B Y, Han X H and Zhang D Z 2000 *Chin. Phys.* **9** 824

[21] Fallman E and Axner O 2003 *Appl. Opt.* **42** 3915

[22] Allen L, Beijersbergen M W, Spreeuw R J C and Woerdman J P 1992 *Phys. Rev.* A **45** 8185